

Published in final edited form as:

Chem Biol. 2012 November 21; 19(11): 1400–1410. doi:10.1016/j.chembiol.2012.09.013.

Hsp104 Drives ‘Protein-Only’ Positive Selection of Sup35 Prion Strains Encoding Strong [*PSI⁺*]

Morgan E. DeSantis^{1,2} and James Shorter^{1,2,*}

¹Department of Biochemistry and Biophysics, University of Pennsylvania, 805b Stellar-Chance Laboratories, 422 Curie Boulevard, Philadelphia, PA 19104, U.S.A

²Biochemistry and Molecular Biophysics Graduate Group, Perelman School of Medicine, University of Pennsylvania, 805b Stellar-Chance Laboratories, 422 Curie Boulevard, Philadelphia, PA 19104, U.S.A

Summary

Structurally distinct, self-templating prion ‘strains’ can encode distinct phenotypes and amplify at different rates depending upon the environment. Indeed, prion strain ensembles can evolve in response to environmental challenges, which makes them highly challenging drug targets. It is not understood how the proteostasis network amplifies one prion strain at the expense of another. Here, we demonstrate that Hsp104 remodels the distinct intermolecular contacts of different synthetic Sup35 prion strains in a way that: selectively amplifies prions encoding strong [*PSI⁺*], and, simultaneously eliminates prions encoding weak [*PSI⁺*]. Hsp104 has reduced ability to fragment prions encoding weak [*PSI⁺*], but readily converts them to non-templating forms. By contrast, Hsp104 readily fragments prions encoding strong [*PSI⁺*], but has reduced ability to eliminate their infectivity. Thus, we illuminate direct mechanisms underpinning how the proteostasis network can drive prion strain selection.

Introduction

Prions are infectious amyloid structures that typically exist as ensembles of multiple structurally distinct, self-templating ‘strains’, which can vary in chemical stability and confer distinct phenotypes (Colby and Prusiner, 2011; Krishnan and Lindquist, 2005; Roberts et al., 2009; Tanaka et al., 2004; Tanaka et al., 2006; Tessier and Lindquist, 2009). As self-replicating structures, prions are hypothesized to be units of selection, i.e. are subject to natural selection (Li et al., 2010; Shorter, 2010; Shorter and Lindquist, 2005; Weissmann, 2012). Thus, natural selection acting at the unfamiliar level of self-templating prions inescapably enriches or depletes various prion strains from strain populations depending upon their conformational fitness, i.e. ability to self-replicate their specific strain conformation under the prevailing environmental conditions (Collinge and Clarke, 2007; Duennwald and Shorter, 2010; Ghaemmaghami et al., 2009; Ghaemmaghami et al., 2011; Li et al., 2010; Roberts et al., 2009; Shorter, 2010; Weissmann, 2012). This microevolutionary process can give rise to conflict between levels of selection (Shorter, 2010). Thus, prions can be detrimental to the individual as with diverse infectious conformers of the mammalian

© 2012 Elsevier Ltd. All rights reserved.

*Correspondence: shorter@mail.med.upenn.edu.

Publisher's Disclaimer: This is a PDF file of an unedited manuscript that has been accepted for publication. As a service to our customers we are providing this early version of the manuscript. The manuscript will undergo copyediting, typesetting, and review of the resulting proof before it is published in its final citable form. Please note that during the production process errors may be discovered which could affect the content, and all legal disclaimers that apply to the journal pertain.

prion protein (PrP), which are connected with fatal neurodegenerative diseases, including Creutzfeldt-Jakob disease (Colby and Prusiner, 2011; Collinge and Clarke, 2007; Weissmann, 2012). Similarly, in yeast, some Sup35 and Ure2 prion strains can be detrimental (McGlinchey et al., 2011). However, in other circumstances, including diverse stress conditions, Sup35 prions and other yeast prions commonly found in wild yeast confer selective advantages and promote the evolution of new traits (Halfmann et al., 2010; Halfmann et al., 2012; Shorter and Lindquist, 2005; Suzuki et al., 2012; True and Lindquist, 2000).

Dramatic examples of prion strain selection are provided by the emergence of drug-resistant strains of PrP and Sup35 in response to specific small molecules (Ghaemmaghami et al., 2009; Li et al., 2010; Roberts et al., 2009; Shorter, 2010). For example, the green tea polyphenol, EGCG, selects for EGCG-resistant strains of Sup35 *in vitro* and *in vivo* (Duennwald and Shorter, 2010; Roberts et al., 2009). Swainsonine selects for drug-resistant mammalian prions in cell culture (Li et al., 2010) and quinacrine selects for drug-resistant mammalian prions in mice (Ghaemmaghami et al., 2009). The ability of prion strain ensembles to evolve in response to environmental challenges created by small molecules makes them challenging drug targets (Shorter, 2010; Weissmann, 2012). Thus, it is critical to understand the endogenous selection pressures within cells and tissues that drive the amplification of one prion strain at the expense of another.

Strain selection phenomena occur in response to the immediate environment. Thus, components of the proteostasis network must play a critical role in strain selection (Balch et al., 2008; Ghaemmaghami et al., 2011; Li et al., 2010). However, little is known or understood about the direct mechanisms by which the proteostasis network selects for or against different prion strains (Collinge and Clarke, 2007; Li et al., 2010; Shorter, 2010). Indeed, the mechanistic interplay between molecular chaperones, prion-remodeling factors, and different amyloid or prion strains is poorly understood at the biochemical and biological level. Here, we exploit the [*PSI⁺*] prion protein, Sup35, to address this issue. Using a minimal system comprised of pure components, we have investigated how various synthetic prion strain ensembles of the translation termination factor, Sup35, which encode different variants of the yeast prion [*PSI⁺*] (Roberts et al., 2009; Shorter, 2010; Shorter and Lindquist, 2005; Tanaka et al., 2004; Tanaka et al., 2006), evolve when challenged with different levels of the prion-remodeling factor, Hsp104.

Hsp104 is a hexameric AAA+ ATPase, which is critical for the propagation of the vast majority of yeast prions (Alberti et al., 2009; Halfmann et al., 2012; Shorter and Lindquist, 2005). How Hsp104 directly affects different Sup35 prion strains is unknown. To address this issue, we exploited pure NM, the prion domain of Sup35 (Figure 1). NM spontaneously assembles into different prion strain ensembles at different temperatures. Thus, prions within strain ensembles formed by synthetic NM at 4°C, termed NM4, possess on average a shorter, less stable amyloid core ($T_m \sim 54^\circ\text{C}$) with distinctive intermolecular contacts (Figure 1). By contrast, synthetic NM prion strain ensembles formed at 25°C or 37°C, termed NM25 and NM37, harbor prions that possess, on average, longer, more stable amyloid cores ($T_m \sim 81^\circ\text{C}$ for NM25 and $T_m \sim 86^\circ\text{C}$ for NM37) with intermolecular contacts distinct to NM4 (Krishnan and Lindquist, 2005; Roberts et al., 2009; Tanaka et al., 2004; Tanaka et al., 2006; Tessier and Lindquist, 2007, 2009; Toyama et al., 2007) (Figure 1). When transformed into [*psi⁻*] yeast cells (which lack Sup35 prions), synthetic NM4 prions confer mostly strong [*PSI⁺*] (strong [*PSI⁺*]:weak [*PSI⁺*] $\sim 3:1$), whereas NM25 and NM37 prions confer mostly weak [*PSI⁺*] (strong [*PSI⁺*]:weak [*PSI⁺*] $\sim 1:3$ for NM25 and $\sim 1:5.7$ for NM37) (Krishnan and Lindquist, 2005; Tanaka et al., 2004; Tanaka et al., 2006) (Figure 1). These mixed distributions of weak and strong [*PSI⁺*] indicate that NM4, NM25, and NM37 are complex mixtures of multiple different prion strain structures, rather than a single pure

strain. Here, 'strength' refers to the magnitude of the translation termination defect caused by depletion of soluble, functional Sup35 by self-templating Sup35 prions (Derkatch et al., 1996; Tanaka et al., 2004). Thus, NM4 prions typically convert more soluble Sup35 to the prion state *in vivo* than NM25 or NM37 prions (Tanaka et al., 2004; Tanaka et al., 2006). It has been suggested that the increased fragility of NM4 compared to NM25, and NM37 enables more facile fragmentation by Hsp104, which generates more fiber ends competent to convert soluble Sup35 to the prion state (Tanaka et al., 2006). However, to the best of our knowledge, this hypothesis has never been tested directly with pure components.

Here, we establish for the first time the direct consequences of Hsp104-catalyzed remodeling on the NM4, NM25, and NM37 ensembles. We define unanticipated differences in the way Hsp104 disrupts the intermolecular contacts of different Sup35 prion strains. This type of mechanistic insight is only possible with Sup35 prions where the intermolecular contacts can be tracked using fluorescence tools that are not yet available for other prions (Krishnan and Lindquist, 2005; Roberts et al., 2009; Wang et al., 2008). We have reconstituted and deciphered the first direct mechanisms by which components of the proteostasis network can drive 'protein only' positive selection of a specific prion strain. Importantly, we verify our findings *in vivo*. Thus, we uncover that Hsp104 directly drives strain selection events that favor prions encoding strong [*PSI*⁺].

Results

Hsp104 more readily remodels NM4 prions than NM25 and NM37

First, we assessed the prion-remodeling activity of Hsp104 against NM4, NM25, and NM37 prions in the presence of Ssa1 (an Hsp70) and Sis1 (an Hsp40) because these molecular chaperones contribute to [*PSI*⁺] propagation *in vivo* (Bagriantsev et al., 2008; Higurashi et al., 2008; Hines et al., 2011; Tipton et al., 2008). Moreover, although Ssa1 and Sis1 are not absolutely required for Hsp104 to remodel Sup35 prions *in vitro*, they can enhance Hsp104 amyloid-remodeling activity (Duennwald et al., 2012; Shorter and Lindquist, 2004, 2006, 2008; Sweeny and Shorter, 2008). Thus, we exposed different synthetic NM prion strain ensembles to increasing concentrations of Hsp104 in the presence of a constant amount of Hsp70 (Ssa1) and Hsp40 (Sis1). We measured prion remodeling using the amyloid-diagnostic dye, Thioflavin-T (ThT), which exhibits enhanced fluorescence upon binding cross-beta amyloid structure (Chernoff et al., 2002). Under our conditions, in the absence of Hsp104 no prion remodeling is observed. Hsp104 more readily remodels NM4 prions than NM25 and NM37 (Figure 2A). The EC₅₀ (the half maximal effective concentration) of Hsp104 was ~0.06 μM for NM4, ~0.12 μM for NM25 and ~0.35 μM for NM37. Very similar EC₅₀ values were obtained when remodeling was measured by the amount of SDS-insoluble NM (SDS-resistance) instead of ThT fluorescence as a measure of fiber integrity (Chernoff et al., 2002) (Figure 2B). The apparent Hill slope (n) became progressively steeper upon moving from NM4 (n~-2.7) to NM25 (n~-4.6) to NM37 (n~-9.8; Figure 2A). These data indicate that Hsp104 functions with increased co-operativity to remodel more stable NM prions, which sequester more primary sequence in cross-beta structure (Figure 1). Thus, to remodel NM37 prions Hsp104 must function with greater co-operativity than to remodel NM4 prions (Figure 2A, B).

In the absence of Ssa1 and Sis1, Hsp104 promoted similar levels of prion remodeling (Figure 2C, D). However, for each strain ensemble the Hsp104 EC₅₀ determined by ThT fluorescence was slightly elevated to ~0.07 μM for NM4, ~0.16 μM for NM25, and ~0.64 μM for NM37 (Figure 2C), and similar values were obtained via SDS-resistance (Figure 2D). By contrast, the apparent Hill slopes were very similar in the presence or absence of Ssa1 and Sis1, which indicates that Ssa1 and Sis1 do not impact Hsp104 co-operativity (Figure 2C, D). The increase in EC₅₀ was most pronounced for NM37 (Figure 2A-D). Thus, Ssa1 and

Sis1 are not absolutely required for Sup35 prion remodeling by Hsp104 (Duennwald et al., 2012; Shorter and Lindquist, 2004, 2006, 2008), but likely play a more important role for Sup35 prions that encode weak [*PSI⁺*]. These findings are consistent with observations that Sis1 depletion only partially impairs [*PSI⁺*] propagation in vivo and that weak [*PSI⁺*] strains are more sensitive to Sis1 depletion than strong [*PSI⁺*] strains (Higurashi et al., 2008; Hines et al., 2011; Tipton et al., 2008).

The reduced ability of Hsp104 to remodel NM37 and NM25 prions compared to NM4 (Figure 2) might reflect a reduced binding affinity for NM37 and NM25 compared to NM4. Yet, the K_d of Hsp104 for NM4, NM25, and NM37 was very similar at ~35nM, ~30nM, and 33nM respectively. Moreover, NM4, NM25, and NM37 all bound similar amounts of Hsp104. Thus, some aspect of NM37 and NM25 prion structure (e.g. increased local stability of the cross-beta form adjacent to where Hsp104 initially engages the prion) likely antagonizes Hsp104 remodeling activity after initial binding.

Hsp104 more readily fragments NM4 prions than NM25 and NM37

To further define how Hsp104 remodels NM4, NM25, and NM37 prions we directly monitored the integrity of their intermolecular prion contacts (Figure 1). To do so, we independently assembled 17 individual single cysteine NM variants labeled with pyrene at different positions. These pyrene-labeled NM variants retain wild-type assembly kinetics and infectivity, indicating that pyrene does not significantly alter prion structure (Krishnan and Lindquist, 2005; Roberts et al., 2009; Wang et al., 2008). Upon intermolecular contact formation, pyrene molecules at select positions, in the Head or Tail (Figure 1), form excimers (excited-state dimers) that produce a strong red shift in fluorescence. Thus, excimer fluorescence reports on intermolecular contact integrity (Krishnan and Lindquist, 2005; Roberts et al., 2009; Wang et al., 2008).

We selected two Hsp104 concentrations to study fragmentation of NM4, NM25, and NM37 strains based on the prion-remodeling data in Figure 2. Thus, we selected a low concentration (0.1 μ M) at which Hsp104 effectively remodeled NM4, but not NM25 or NM37 (Figure 2). We also assessed a high concentration (1 μ M) at which Hsp104 had maximal activity against NM4, NM25, and NM37 (Figure 2). Treatment of preformed pyrene-labeled NM4, NM25, or NM37 prions with buffer or Ssa1 and Sis1 alone had no effect on prion contacts (Figure 3). By contrast, addition of a low concentration (0.1 μ M) of Hsp104 readily disrupted both the Head (residues 21–38) and Tail (residues 79–96) contacts of NM4 prions in the presence or absence of Ssa1 and Sis1 (Figure 3). Thus, Hsp104 can readily break intermolecular prion contacts, which are remarkably stable and resist external pulling forces of ~250pN (Dong et al., 2010).

Likewise, in the presence or absence of Ssa1 and Sis1, low concentrations of Hsp104 readily disrupted the Tail contacts (residues 91–106) of NM25 prions. However, in contrast to NM4, the Head contacts (residues 21–38) of NM25 prions were more refractory to disruption by low concentrations of Hsp104 (Figure 3). This effect was even more pronounced for NM37 prions, where a low concentration of Hsp104 (0.1 μ M) was even less able to disrupt the Head (residues 21–38) and Tail (residues 91–112) contacts (Figure 3). For NM37 prions, the presence of Ssa1 and Sis1 was more critical, and enhanced the ability of a low concentration of Hsp104 (0.1 μ M) to disrupt Tail contacts (Figure 3). These data suggest that Hsp104 more readily fragments NM4 prions than NM25 prions, which in turn are more readily fragmented than NM37 prions.

These data also indicate that propagation of strong [*PSI⁺*] in vivo likely proceeds via Hsp104-catalyzed severing of both Head and Tail prion contacts, as observed with NM4 prions in vitro (Figure 3). By contrast, propagation of weak [*PSI⁺*] in vivo likely proceeds

via Hsp104-catalyzed severing of predominantly the Tail contact, as observed with NM25 and NM37 prions (Figure 3). Moreover, these data suggest that at a low concentration (0.1 μ M), Hsp104 can break the Tail contacts of NM25 and NM37 prions (Figure 3) without causing large reductions in the total amount of cross-beta structure as determined by ThT fluorescence or SDS-resistance (Figure 2A–D). Thus, prion fragmentation (i.e. breakage of intermolecular contacts) can be separated from prion remodeling (i.e. reductions in the amount of cross-beta structure measured by ThT fluorescence or SDS-resistance).

Electron microscopy (EM) confirmed that at this low concentration (0.1 μ M), Hsp104 fragmented networks of NM4 prions more readily than NM25 or NM37 prions in the presence or absence of Ssa1 and Sis1 (Figure 4, compare conditions without Hsp104 to those with 0.1 μ M Hsp104). This increased fragmentation of NM4 by Hsp104 is due to breakage of both Head and Tail contacts (Figure 3), which yields more fiber ends able to capture and convert non-prion forms of Sup35. The enhanced severing of NM4 prions by Hsp104 helps explain why they encode predominantly strong [*PSI⁺*] and why NM25 and NM37 prions encode predominantly weak [*PSI⁺*] in vivo.

High levels of Hsp104 convert NM25 and NM37 to non-templating structures

Hsp104 overexpression cures weak [*PSI⁺*] more readily than strong [*PSI⁺*] (Chernoff et al., 1995; Wegrzyn et al., 2001), yet NM25 and NM37 were more refractory to Hsp104-catalyzed remodeling than NM4 (Figure 2A–D). Indeed, elevated levels of Hsp104 have differential ability to cure various prions in vivo. For example, Hsp104 overexpression cures [*PSI⁺*] but has limited ability to cure [*URE3*] (Chernoff et al., 1995; Kryndushkin et al., 2008; Moriyama et al., 2000). Yet in vitro, Hsp104 catalyzes similar amounts of Sup35 and Ure2 prion remodeling (Shorter and Lindquist, 2006). Importantly, however, when the in vitro Hsp104-remodeled Sup35 and Ure2 products are compared functionally, Sup35 products fail to seed prion assembly and do not convert [*psi⁻*] cells to [*PSI⁺*], whereas the Ure2 products are short prion fibers with high infectivity that readily convert [*ure-0*] cells to [*URE3*] (Shorter and Lindquist, 2006). Based on this precedent, we hypothesized that NM4 prions that had been remodeled by Hsp104 might retain greater seeding activity than NM25 or NM37 prions that had been remodeled by Hsp104.

Remodeling of NM4 prions by a high concentration (1 μ M) of Hsp104 in the presence or absence of Ssa1 and Sis1 led to increased breakage of Head and Tail contacts (Figure 3). However, intermolecular contacts were still detectable (Figure 3). Surprisingly, EM revealed that NM4 prions were converted to numerous short fibers by high levels of Hsp104 (Figure 4, conditions with 1 μ M Hsp104). By contrast, remodeling of NM25 and NM37 prions by a high concentration (1 μ M) of Hsp104, in the presence or absence of Ssa1 and Sis1, led to more effective disruption of Head and Tail contacts compared to NM4 (Figure 3). Indeed, very few fibers were visible by EM after NM25 prions were remodeled by high concentrations of Hsp104 (Figure 4, conditions with 1 μ M Hsp104). The predominant reaction products were small soluble species although occasional amorphous structures were also observed (Figure 4 arrows, 1 μ M Hsp104). Similar types of amorphous structures were more commonly observed after remodeling NM37 prions with high concentrations of Hsp104 (Figure 4 arrows, 1 μ M Hsp104). Presumably, these structures can still bind ThT and retain some SDS-resistance (Figure 2A–D). Taken together, these findings suggest that even at high concentrations, Hsp104 fragments NM4 into shorter and shorter fibers. By contrast, acting at high concentrations, Hsp104 effectively disrupts the Head and Tail contacts of NM25 and NM37 prions (Figure 3), but simultaneously converts them into a mixture of soluble species and alternative aggregated structures (Figure 4).

Next, we compared the self-templating activity of NM4, NM25, and NM37 prions that had been treated with a low (0.1 μ M) or high concentration (1 μ M) of Hsp104 in the presence or

absence of Ssa1 and Sis1. To do so, we used His₆-Hsp104, which could be rapidly depleted at the end of the reaction using Ni-sepharose without co-depleting NM prions (Shorter and Lindquist, 2004, 2006). After depleting His₆-Hsp104, we tested the ability of the remaining conformers to seed the polymerization of soluble NM *in vitro*. In the presence of Ssa1 and Sis1, treatment with a low concentration of Hsp104 increased the ability of NM4, NM25, and NM37 prions to seed the polymerization of soluble NM (Figure 5A–C, compare dark blue to grey lines). This effect was more pronounced for NM4 prions (Figure 5A) than for NM25 prions (Figure 5B). Indeed, treatment with a low concentration of Hsp104 mimicked the effect of sonication for NM4 (Figure 5A, compare black to grey lines). By contrast, the low concentration of Hsp104 was not as effective as sonication in generating new fiber ends for NM25 (Figure 5B, compare black to grey lines). Hsp104 was least effective in generating new fiber ends for NM37 (Figure 5C, compare black to grey lines). For NM4 and NM25, we obtained very similar results if Ssa1 and Sis1 were omitted (Figure 5D, E). By contrast, for NM37, treatment with a low concentration of Hsp104 did not increase the ability of NM37 to seed soluble NM (Figure 5F, compare dark blue to orange lines). Thus, Ssa1 and Sis1 play a more important role in Hsp104-catalyzed fragmentation of NM37 prions. Taken together, these data suggest that Hsp104 more readily fragments NM4 than NM25. Moreover, they suggest that NM37 prions are more resistant to Hsp104-catalyzed fragmentation, and make a more stringent requirement for Ssa1 and Sis1. Thus, as cross-beta structure encroaches deeper into C-terminal stretches of primary sequence, as with NM25 and NM37 (Figure 1), then NM prions become more difficult for Hsp104 to fragment.

Hsp104 selectively amplifies prions that encode strong [*PSI⁺*]

Next, we determined how treatment with a low concentration of Hsp104 affected the composition of the strain distribution that underpins the NM4 ensemble (Figure 1). Thus, we transformed reaction products into [*psi⁻*] cells (Shorter and Lindquist, 2006; Tanaka et al., 2004). Transformation of [*psi⁻*] cells with unsonicated NM4 yielded a mixture of strong [*PSI⁺*] (~30%), weak [*PSI⁺*] (~10%), and [*psi⁻*] (~60%) colonies, whereas sonicated NM4 yielded strong [*PSI⁺*] (~60%), weak [*PSI⁺*] (~20%), and [*psi⁻*] (~20%) (Figure 6A). Thus, sonication increased the proportion of total [*PSI⁺*] colonies without affecting the strong [*PSI⁺*]:weak [*PSI⁺*] ratio, which remained at ~3:1 (Figure 6A). By contrast, incubation of NM4 with a low Hsp104 concentration yielded a mixture of strong [*PSI⁺*] (~81%), weak [*PSI⁺*] (~10%), and [*psi⁻*] (~9%) colonies (Figure 6A). Thus, like sonication, Hsp104 increased the proportion of total [*PSI⁺*] colonies. However, in contrast to sonication, Hsp104 shifted the strong [*PSI⁺*]:weak [*PSI⁺*] ratio to ~8:1 (Figure 6A). We obtained very similar results when Ssa1 and Sis1 were omitted, and treatment with Ssa1 and Sis1 alone did not change the strain distribution (Figure 6A). Thus, exposure to a low concentration of Hsp104 preferentially amplifies prions encoding strong [*PSI⁺*].

Prions that encode strong [*PSI⁺*] were also amplified upon treating NM25 and NM37 prions with a low concentration of Hsp104 (Figure 6B, C). Thus, like sonication, treatment of NM25 prions with a low Hsp104 concentration (0.1 μM) in the presence or absence of Ssa1 and Sis1 increased the proportion of total [*PSI⁺*] colonies from ~29% to ~80% (Figure 6B). For NM37, sonication increased the proportion of total [*PSI⁺*] colonies from ~20% to ~60%, whereas treatment with a low Hsp104 concentration in the presence of Ssa1 and Sis1 increased it to ~31% (Figure 6C). In the absence of Ssa1 and Sis1, treatment of NM37 with a low Hsp104 concentration only slightly increased the proportion of total [*PSI⁺*] colonies (Figure 6C). Sonication maintained the strong [*PSI⁺*]:weak [*PSI⁺*] ratio at ~1:3 for NM25 and ~1:5 for NM37 (Figure 6B, C). By contrast, for both NM25 and NM37, treatment with a low concentration of Hsp104 in the presence of Ssa1 and Sis1 shifted the strong [*PSI⁺*]:weak [*PSI⁺*] ratio toward strong [*PSI⁺*] (Figure 6B, C). Specifically, Hsp104 shifted the strong [*PSI⁺*]:weak [*PSI⁺*] ratio from ~1:3 to ~1:1.4 for NM25 and from ~1:5 to ~1:1.6 for NM37

(Figure 6B, C). We obtained very similar results when Ssa1 and Sis1 were omitted for NM25: the strong [*PSI⁺*]:weak [*PSI⁺*] ratio shifted to ~1:1.2 (Figure 6B). However, for NM37, omission of Ssa1 and Sis1 led to a smaller shift in the strong [*PSI⁺*]:weak [*PSI⁺*] from ~1:5 to ~1:2.2 (Figure 6C). Treatment with Ssa1 and Sis1 alone did not change the strain distribution (Figure 6B, C). Collectively, these findings suggest that Hsp104-catalyzed prion fragmentation is strain selective, whereas sonication is non-specific. Remarkably, when NM prion strain ensembles are exposed to low concentrations of Hsp104, prions encoding strong [*PSI⁺*] were selectively amplified and prions encoding weak [*PSI⁺*] were selected against.

Hsp104 selectively eliminates prions that encode weak [*PSI⁺*]

Next, we assessed the behavior of NM4, NM25, and NM37 prions that had been exposed to a high concentration of Hsp104 (1 μ M) in the presence of Ssa1 and Sis1 for 60min. Here, Hsp104 diminished the ability of NM25 and NM37 to seed the polymerization of soluble NM in vitro (Figure 5B, C, compare dark blue to green line) and diminished their ability to transform [*psi⁻*] cells to weak [*PSI⁺*] (Figure 6B, C). Indeed, no weak [*PSI⁺*] colonies were recovered after treating NM37 with high concentrations of Hsp104 (Figure 6C). Remarkably, however, NM25 and NM37 remodeled products could still induce some strong [*PSI⁺*] colonies (Figure 6B, C). By contrast, the final NM4 reaction products retained a greater ability to seed the polymerization of soluble NM in vitro (Figure 5A, compare dark blue and green line) and could still transform [*psi⁻*] cells to strong [*PSI⁺*], but not weak [*PSI⁺*] (Figure 6A). We obtained very similar results when Ssa1 and Sis1 were omitted, and treatment with Ssa1 and Sis1 alone had no effect (Figure 5D–F, 6A–C). These data suggest that elevated levels of Hsp104 preferentially convert NM25 and NM37 prions, which encode predominantly weak [*PSI⁺*], to non-prion forms, whereas a subpopulation of remodeled NM4 products retain their strong [*PSI⁺*] prion character. These data are sufficient to explain why overexpression of Hsp104 cures weak [*PSI⁺*] more readily than strong [*PSI⁺*] (Chernoff et al., 1995; Wegrzyn et al., 2001), because Hsp104-catalyzed remodeling preferentially destroys the prion nature of NM25 and NM37 prions, but not NM4 prions.

Next, we assessed whether prions encoding strong [*PSI⁺*] could sweep the population after treating NM37 with a high concentration of Hsp104 for 60min in the presence of Ssa1 and Sis1. To do so, we used a larger quantity of the reaction products to seed (50% wt/wt) NM assembly at 4°C for 6h. Strikingly, we recovered prions that encoded purely strong [*PSI⁺*] (Figure 6D). By contrast, if sonication were used instead of Hsp104 then the prion ensemble retained the original strain distribution that was strongly biased toward weak [*PSI⁺*] (Figure 6D). Thus, Hsp104 selectively amplifies prions that encode strong [*PSI⁺*] and selectively eliminates prions that encode weak [*PSI⁺*].

Hsp104 selects against prions that encode weak [*PSI⁺*] in vivo

Finally, we corroborated these findings in vivo in two ways. First, we induced [*PSI⁺*] by expressing high levels of NM-YFP in yeast expressing normal or elevated levels of Hsp104. [*PSI⁺*] induction was reduced from ~26% to ~5% in cells expressing high levels of Hsp104 (Figure 7A). Strikingly, however, this effect was largely due to a decrease in the appearance of weak [*PSI⁺*] colonies. Indeed, the proportion of colonies that were strong [*PSI⁺*] decreased from ~6.7% in the vector control to ~3.3% in cells overexpressing Hsp104, which was not statistically significant ($p=0.2521$, two-tailed Student's *t* test). By contrast, the proportion of colonies that were weak [*PSI⁺*] decreased from ~19.3% in the vector control to ~1.7% in cells overexpressing Hsp104, which was statistically significant ($p=0.0006$, two-tailed Student's *t* test; Figure 7A). Thus, Hsp104 selectively antagonizes the induction of weak [*PSI⁺*] in vivo.

In a second approach, we induced $[PSI^+]$ by transforming synthetic NM4, NM25, or NM37 prions into $[psi^-]$ cells expressing normal or elevated levels of Hsp104. Here too, although high levels of Hsp104 reduced $[PSI^+]$ induction, this effect was largely due to a reduction in the proportion of weak $[PSI^+]$ colonies (Figure 7B). Indeed, the reduction in weak $[PSI^+]$ induction caused by Hsp104 overexpression was ~4.3-fold for NM4 ($p=0.0073$, two-tailed Student's t test), ~29-fold for NM25 ($p<0.0001$, two-tailed Student's t test), and ~13-fold for NM37 infection ($p=0.0013$, two-tailed Student's t test), whereas the reduction in strong $[PSI^+]$ induction was ~1.6-fold for NM4 ($p=0.0033$, two-tailed Student's t test), ~1.1-fold for NM25 ($p=0.5896$, two-tailed Student's t test), and ~1.5-fold for NM37 infection ($p=0.3098$, two-tailed Student's t test). Thus, the reduction in weak $[PSI^+]$ induction caused by elevated Hsp104 levels was statistically significant for NM4, NM25, and NM37 infection, whereas the reduction in strong $[PSI^+]$ induction only reached statistical significance for NM4 infection. These data suggest that Hsp104 selects against Sup35 prions that encode weak $[PSI^+]$ in vitro and in vivo.

Discussion

To the best of our knowledge, our study represents the first reconstitution of direct mechanisms by which the chaperone network can drive 'protein only' positive selection of a specific prion strain in vitro and in vivo. Thus, we uncover that Hsp104 remodeling activity creates a positive selection pressure for Sup35 prion strains that encode strong $[PSI^+]$. We also assessed how Hsp104 impacts the distinct intermolecular contacts of different synthetic Sup35 prion strains. At low concentrations, Hsp104 more readily fragments Sup35 prion strains encoding strong $[PSI^+]$ by breaking both Head and Tail contacts, thereby liberating more polymerization surfaces for further conformational replication. This observation suggests that the precise Sup35 prion conformation determines the fragmentation rate by Hsp104, which in turn makes a large contribution to determining the strength of the $[PSI^+]$ -encoded nonsense suppression phenotype.

Unexpectedly, the increased fragmentation of prion conformations that encode strong $[PSI^+]$ does not lead to increased elimination of the prion form, even at high Hsp104 concentrations. One possible explanation is that the increased number of fiber ends breaches a threshold that converts newly liberated soluble NM to the prion form with kinetics that keeps pace with Hsp104-catalyzed release of soluble NM. By contrast, Hsp104 is much less able to fragment prion strains (NM25 or NM37) that encode weak $[PSI^+]$. Indeed, acting at low concentrations Hsp104 preferentially fragments the Tail contact of NM25 and NM37 prions. Moreover, for NM37 prions, Ssa1 and Sis1 are more stringently required to break the Tail contact. Consequently, treatment of NM25 and NM37 prions with low Hsp104 concentrations yields fewer ends for conformational replication compared to strains that encode strong $[PSI^+]$. At high concentrations, Hsp104 converts NM25 and NM37 prions to soluble species and non-templating amorphous aggregates, which lack seeding activity.

Our findings also suggest that Hsp104 activity can create a selection pressure against Sup35 prions that encode weak $[PSI^+]$ both in vitro and in vivo. These findings help explain why some weak $[PSI^+]$ strains spontaneously convert to strong $[PSI^+]$ (Kochneva-Pervukhova et al., 2001). Thus, prions encoding strong $[PSI^+]$ that spontaneously appear in a weak $[PSI^+]$ strain would be rapidly and selectively amplified by Hsp104 acting even at low concentrations. Sup35 prions encoding strong $[PSI^+]$ would then sweep the Sup35 prion population of that cell. In this way, Hsp104 drives 'protein only' directional selection for Sup35 prions that encode strong $[PSI^+]$.

Unlike their mammalian counterparts, yeast prions confer advantages to their host and enable the rapid evolution of beneficial, heritable traits in response to environmental stress

(Alberti et al., 2009; Halfmann et al., 2012; Suzuki et al., 2012; True et al., 2004; Tyedmers et al., 2008). Indeed, $[PSI^+]$, and numerous other prions are found in natural populations of yeast (Halfmann et al., 2012). $[PSI^+]$ induction frequency increases in response to various environmental stresses despite elevated Hsp104 expression levels (Tyedmers et al., 2008). Our data suggest that elevated Hsp104 concentration might help ensure the appearance of strong $[PSI^+]$ rather than weak $[PSI^+]$ in response to environmental stress. The appearance of strong $[PSI^+]$ would then in turn release larger amounts of cryptic genetic variation in a more stable, heritable manner, which could facilitate more rapid sampling of diverse phenotypes within the population and promote survival (Shorter, 2010; Shorter and Lindquist, 2005; True et al., 2004). Our data provide important mechanistic insights into how prion-remodeling components of the proteostasis network directly drive the Darwinian evolution of prion strains (Li et al., 2010). An understanding of how the proteostasis network affects the evolution of mammalian prion strain ensembles is urgently needed to help combat the devastating neurodegenerative disorders inflicted by these evolvable infectious agents (Collinge and Clarke, 2007; Shorter, 2010). Moreover, the prion concept has now expanded to explain how self-templating amyloid forms might spread in various neurodegenerative amyloidoses, including Alzheimer's and Parkinson's disease (Cushman et al., 2010). In these cases too, it is likely that strain phenomena are at play, and it is critical to understand how the proteostasis network might affect strain selection events of various self-templating amyloid forms connected to neurodegeneration (Cushman et al., 2010; Duennwald and Shorter, 2010; Shorter, 2010).

Significance

The endogenous selection pressures within cells and tissues that drive the amplification of one prion strain at the expense of another are not understood. Here, using pure components, we define for the first time the direct effects of Hsp104 on different synthetic Sup35 prion strains, which were previously unknown. Hsp104 more readily remodels (i.e. reduces the amount of cross-beta structure) Sup35 prions with shorter, less stable amyloid cores that encode strong $[PSI^+]$. Counterintuitively, this enhanced remodeling favors the replication of Sup35 prions that encode strong $[PSI^+]$. We define unanticipated differences in the way Hsp104 disrupts the intermolecular contacts of different Sup35 prion strains. Thus, at low concentrations, Hsp104 can effectively break Head and Tail contacts of prions encoding strong $[PSI^+]$, but can only break the Tail contact of prions encoding weak $[PSI^+]$. Indeed, Hsp104 can fragment Sup35 prions by breaking the Tail contact without remodeling cross-beta structure (i.e. reducing ThT fluorescence or the amount of SDS-resistant Sup35). Ssa1 (Hsp70) and Sis1 (Hsp40) are more stringently required for Hsp104 to break intermolecular contacts of Sup35 prions encoding weak $[PSI^+]$. Collectively, these findings explain why particular Sup35 prion strains encode strong $[PSI^+]$ and why others encode weak $[PSI^+]$ in vivo. At higher concentrations, Hsp104 more effectively disrupts the intermolecular contacts of prions encoding weak $[PSI^+]$ by converting prions into non-templating structures. By contrast, even though Hsp104 more readily fragments prions encoding strong $[PSI^+]$ it has reduced ability to eliminate their infectivity. These findings explain why overexpression of Hsp104 cures weak $[PSI^+]$ more readily than strong $[PSI^+]$ in vivo. Our findings represent the first reconstitution of 'protein-only' positive selection of a specific prion strain by a molecular chaperone (Hsp104). Moreover, these data have key ramifications for eliminating deleterious, evolvable mammalian prions and other self-templating amyloid conformers connected to devastating neurodegenerative diseases.

Experimental Procedures

Proteins

Hsp104, Ssa1, Sis1 and NM were purified as described (Shorter and Lindquist, 2004, 2006, 2008; Sweeny et al., 2011). Single cysteine NM mutants were labeled with pyrene-maleimide (Invitrogen) under denaturing conditions as described (Krishnan and Lindquist, 2005). The purity of all proteins was >95% as determined by SDS-PAGE and Coomassie staining. Hsp104 concentrations refer to the hexamer concentration.

Prion assembly

NM (5 μ M) fibers were assembled in Assembly Buffer (AB: 40mM HEPES-KOH pH 7.4, 150mM KCl, 20mM MgCl₂ and 1mM DTT) for 16h with agitation (1,400rpm in an Eppendorf Thermomixer) at 4°C to yield NM4, at 25°C to yield NM25, or at 37°C to yield NM37 (Roberts et al., 2009). All fiber preparations were assessed by Thioflavin-T (ThT) fluorescence, SDS-resistance, and electron microscopy (Chernoff et al., 2002; Shorter and Lindquist, 2004, 2006). Fibers were diluted to the requisite concentration for subsequent remodeling reactions. Alternatively, NM proteins (5 μ M) carrying pyrene labels at the indicated single cysteine were assembled at 4°C, 25°C, or 37°C with agitation for 12h.

Prion remodeling

NM4, NM25, or NM37 (2.5 μ M) were incubated with increasing concentrations of Hsp104 (0.001–25 μ M) in the presence or absence of Ssa1 (2.5 μ M) and Sis1 (2.5 μ M) for 60min at 25°C in AB in the presence of ATP (5mM) and an ATP regeneration system (1mM creatine phosphate, 0.25 μ M creatine kinase (Roche)). Fiber integrity was then determined by ThT fluorescence, SDS-resistance, or electron microscopy (Chernoff et al., 2002; Shorter and Lindquist, 2004, 2006). To monitor intermolecular prion contacts, we employed NM prions labeled with pyrene at the indicated single cysteine as described (Krishnan and Lindquist, 2005). Pyrene excimer fluorescence was measured as described (Krishnan and Lindquist, 2005).

Hsp104:NM prion binding

Due to rapid ATP hydrolysis, Hsp104 engages substrates transiently. Thus, to assess Hsp104:NM prion binding interactions we employed conditions where ATP hydrolysis was restricted. Thus, we employed wild-type Hsp104 in the presence of ATP γ S (1mM). Increasing amounts of Hsp104 were incubated with NM4, NM25, or NM37 (0.5 μ M monomer) in binding buffer (40mM HEPES-KOH pH 7.4, 150mM KCl, 20mM MgCl₂ and 1mM DTT) for 10min on ice. NM4, NM25, or NM37 was then rapidly recovered by centrifugation at 100,000g for 10min. Pellets were washed gently twice with binding buffer and the amount of Hsp104 recovered in the pellet fraction was determined by quantitative immunoblot and densitometry in comparison to Hsp104 reference curves.

Seeded NM assembly reactions

NM4, NM25, or NM37 (2.5 μ M monomer) in AB were either left untreated, sonicated, or treated with His₆-Hsp104 (0.1 μ M or 1 μ M), Ssa1 (2.5 μ M) and Sis1 (2.5 μ M) for 60min at 25°C as above. Reactions were then depleted of His₆-Hsp104 as described (Shorter and Lindquist, 2004) and used to seed (2% wt/wt) fresh, undisturbed NM (2.5 μ M) polymerization in seeding buffer (40mM HEPES-KOH pH 7.4, 150mM NaCl, 1mM DTT, 20mM EDTA). Seeding reactions were performed at 4°C for NM4 products, 25°C for NM25 products, and 37°C for NM37 products (in Figure 5). Alternatively (for Figure 6D), NM37 (2.5 μ M monomer) in AB was either left untreated, sonicated, or treated with His₆-Hsp104 (1 μ M), Ssa1 (2.5 μ M) and Sis1 (2.5 μ M) for 60min at 25°C. Reactions were then

depleted of His₆-Hsp104 as described (Shorter and Lindquist, 2004) and used to seed (50% wt/wt) fresh, undisturbed NM (2.5μM) polymerization at 4°C for 6h in seeding buffer. Owing to the transience of Hsp104-substrate interactions, NM conformers are not co-depleted with Hsp104 (Shorter and Lindquist, 2004, 2006).

NM prion transformation

Yeast cells from a W303-derived strain (*MATa leu2-3, -112 his3-11 trp1-1 ura3-1 ade1-14 can1-100 [pin⁻] [psi⁻] [ure-o]*) that contained an *ADE1* nonsense mutation suppressible by [*PSI⁺*] were transformed with the indicated NM conformers and a *URA3* plasmid as described (Krishnan and Lindquist, 2005; Shorter and Lindquist, 2006). The proportion of Ura⁺ transformants that acquired weak or strong [*PSI⁺*] was then determined. In some experiments (Figure 7B), the [*psi⁻*] yeast cells harbored a plasmid carrying *HSP104* under the control of a galactose-inducible promoter or an empty vector control. In this case, cells were grown in selective SGal media prior to transformation. Thus, as soon as the synthetic prions entered the cytoplasm they are exposed to high levels of Hsp104. Immediately after prion transformation, cells were plated on SD-ura media to switch off expression from the *HSP104* plasmid.

[*PSI⁺*] induction

Yeast cells from a W303-derived strain (*MATa leu2-3, -112 his3-11 trp1-1 ura3-1 ade1-14 can1-100 [PIN⁺] [psi⁻] [ure-o]*) were transformed with a plasmid that encoded *NM-YFP* under the control of a galactose-inducible promoter and either an empty vector control or a plasmid with *HSP104* under the control of a galactose-inducible promoter. Cells were grown in selective liquid medium containing raffinose as sole carbon source over night. The next day, the yeast cells were washed three times with sterile water before transferring them to selective liquid media containing galactose as the sole carbon source. The cells were incubated in the galactose media for 6h at 30°C before they were diluted to an OD600 of 0.002 and evenly plated on 25% YPD plates. The proportion of red ([*psi⁻*] colonies), white (strong [*PSI⁺*] colonies), and pink (weak [*PSI⁺*] colonies) ADE⁺ colonies was then determined.

Acknowledgments

We thank Susan Lindquist for generous provision of reagents and Aaron Gitler for critiques. These studies were supported by: a Chemistry-Biology Interface Fellowship from NIH grant 2T32GM071339; a Ruth L. Kirschstein National Research Service Award 1F31NS079009 (to M.E.D.); an NIH Director's New Innovator Award 1DP2OD002177; and an Ellison Medical Foundation New Scholar in Aging Award (to J.S.).

References

- Alberti S, Halfmann R, King O, Kapila A, Lindquist S. A systematic survey identifies prions and illuminates sequence features of prionogenic proteins. *Cell*. 2009; 137:146–158. [PubMed: 19345193]
- Bagriantsev SN, Gracheva EO, Richmond JE, Liebman SW. Variant-specific [*PSI⁺*] infection is transmitted by Sup35 polymers within [*PSI⁺*] aggregates with heterogeneous protein composition. *Mol Biol Cell*. 2008; 19:2433–2443. [PubMed: 18353968]
- Balch WE, Morimoto RI, Dillin A, Kelly JW. Adapting proteostasis for disease intervention. *Science*. 2008; 319:916–919. [PubMed: 18276881]
- Chernoff YO, Lindquist SL, Ono B, Inge-Vechtomov SG, Liebman SW. Role of the chaperone protein Hsp104 in propagation of the yeast prion-like factor [*PSI⁺*]. *Science*. 1995; 268:880–884. [PubMed: 7754373]
- Chernoff YO, Uptain SM, Lindquist SL. Analysis of prion factors in yeast. *Methods Enzymol*. 2002; 351:499–538. [PubMed: 12073366]

- Colby DW, Prusiner SB. De novo generation of prion strains. *Cold Spring Harb Perspect Biol.* 2011; 3:a006833. [PubMed: 21421910]
- Collinge J, Clarke AR. A general model of prion strains and their pathogenicity. *Science.* 2007; 318:930–936. [PubMed: 17991853]
- Cushman M, Johnson BS, King OD, Gitler AD, Shorter J. Prion-like disorders: blurring the divide between transmissibility and infectivity. *J Cell Sci.* 2010; 123:1191–1201. [PubMed: 20356930]
- Derkatch IL, Chernoff YO, Kushnirov VV, Inge-Vechtomov SG, Liebman SW. Genesis and variability of [*PSI⁺*] prion factors in *Saccharomyces cerevisiae*. *Genetics.* 1996; 144:1375–1386. [PubMed: 8978027]
- Dong J, Castro CE, Boyce MC, Lang MJ, Lindquist S. Optical trapping with high forces reveals unexpected behaviors of prion fibrils. *Nat Struct Mol Biol.* 2010; 17:1422–1430. [PubMed: 21113168]
- Duennwald ML, Echeverria A, Shorter J. Small heat shock proteins potentiate amyloid dissolution by protein disaggregases from yeast and humans. *PLoS Biol.* 2012; 10:e1001346. [PubMed: 22723742]
- Duennwald ML, Shorter J. Countering amyloid polymorphism and drug resistance with minimal drug cocktails. *Prion.* 2010; 4:244–251. [PubMed: 20935457]
- Ghaemmaghami S, Ahn M, Lessard P, Giles K, Legname G, DeArmond SJ, Prusiner SB. Continuous quinacrine treatment results in the formation of drug-resistant prions. *PLoS Pathog.* 2009; 5:e1000673. [PubMed: 19956709]
- Ghaemmaghami S, Watts JC, Nguyen HO, Hayashi S, DeArmond SJ, Prusiner SB. Conformational transformation and selection of synthetic prion strains. *J Mol Biol.* 2011; 413:527–542. [PubMed: 21839745]
- Halfmann R, Alberti S, Lindquist S. Prions, protein homeostasis, and phenotypic diversity. *Trends Cell Biol.* 2010; 20:125–133. [PubMed: 20071174]
- Halfmann R, Jarosz DF, Jones SK, Chang A, Lancaster AK, Lindquist S. Prions are a common mechanism for phenotypic inheritance in wild yeasts. *Nature.* 2012; 482:363–368. [PubMed: 22337056]
- Higurashi T, Hines JK, Sahi C, Aron R, Craig EA. Specificity of the J-protein Sis1 in the propagation of 3 yeast prions. *Proc Natl Acad Sci USA.* 2008; 105:16596–16601. [PubMed: 18955697]
- Hines JK, Higurashi T, Srinivasan M, Craig EA. Influence of prion variant and yeast strain variation on prion-molecular chaperone requirements. *Prion.* 2011; 5:238–244. [PubMed: 22156732]
- Kochneva-Pervukhova NV, Chechenova MB, Valouev IA, Kushnirov VV, Smirnov VN, Ter-Avanesyan MD. [*PSI⁺*] prion generation in yeast: characterization of the ‘strain’ difference. *Yeast.* 2001; 18:489–497. [PubMed: 11284005]
- Krishnan R, Lindquist SL. Structural insights into a yeast prion illuminate nucleation and strain diversity. *Nature.* 2005; 435:765–772. [PubMed: 15944694]
- Kryndushkin DS, Shewmaker F, Wickner RB. Curing of the [*URE3*] prion by Btn2p, a Batten disease-related protein. *EMBO J.* 2008; 27:2725–2735. [PubMed: 18833194]
- Li J, Browning S, Mahal SP, Oelschlegel AM, Weissmann C. Darwinian evolution of prions in cell culture. *Science.* 2010; 327:869–872. [PubMed: 20044542]
- McGlinchey RP, Kryndushkin D, Wickner RB. Suicidal [*PSI⁺*] is a lethal yeast prion. *Proc Natl Acad Sci USA.* 2011; 108:5337–5341. [PubMed: 21402947]
- Moriyama H, Edskes HK, Wickner RB. [*URE3*] prion propagation in *Saccharomyces cerevisiae*: requirement for chaperone Hsp104 and curing by overexpressed chaperone Ydj1p. *Mol Cell Biol.* 2000; 20:8916–8922. [PubMed: 11073991]
- Roberts BE, Duennwald ML, Wang H, Chung C, Lopreiato NP, Sweeny EA, Knight MN, Shorter J. A synergistic small-molecule combination directly eradicates diverse prion strain structures. *Nat Chem Biol.* 2009; 5:936–946. [PubMed: 19915541]
- Shorter J. Emergence and natural selection of drug-resistant prions. *Mol Biosyst.* 2010; 6:1115–1130. [PubMed: 20422111]
- Shorter J, Lindquist S. Hsp104 catalyzes formation and elimination of self-replicating Sup35 prion conformers. *Science.* 2004; 304:1793–1797. [PubMed: 15155912]

- Shorter J, Lindquist S. Prions as adaptive conduits of memory and inheritance. *Nat Rev Genet.* 2005; 6:435–450. [PubMed: 15931169]
- Shorter J, Lindquist S. Destruction or potentiation of different prions catalyzed by similar Hsp104 remodeling activities. *Mol Cell.* 2006; 23:425–438. [PubMed: 16885031]
- Shorter J, Lindquist S. Hsp104, Hsp70 and Hsp40 interplay regulates formation, growth and elimination of Sup35 prions. *EMBO J.* 2008; 27:2712–2724. [PubMed: 18833196]
- Suzuki G, Shimazu N, Tanaka M. A yeast prion, Mod5, promotes acquired drug resistance and cell survival under environmental stress. *Science.* 2012; 336:355–359. [PubMed: 22517861]
- Sweeny EA, DeSantis ME, Shorter J. Purification of Hsp104, a protein disaggregase. *J Vis Exp.* 2011; 55:e3190.
- Sweeny EA, Shorter J. Prion proteostasis: Hsp104 meets its supporting cast. *Prion.* 2008; 2:135–140. [PubMed: 19242125]
- Tanaka M, Chien P, Naber N, Cooke R, Weissman JS. Conformational variations in an infectious protein determine prion strain differences. *Nature.* 2004; 428:323–328. [PubMed: 15029196]
- Tanaka M, Collins SR, Toyama BH, Weissman JS. The physical basis of how prion conformations determine strain phenotypes. *Nature.* 2006; 442:585–589. [PubMed: 16810177]
- Tessier PM, Lindquist S. Prion recognition elements govern nucleation, strain specificity and species barriers. *Nature.* 2007; 447:556–561. [PubMed: 17495929]
- Tessier PM, Lindquist S. Unraveling infectious structures, strain variants and species barriers for the yeast prion [*PSI⁺*]. *Nat Struct Mol Biol.* 2009; 16:598–605. [PubMed: 19491937]
- Tipton KA, Verges KJ, Weissman JS. In vivo monitoring of the prion replication cycle reveals a critical role for Sis1 in delivering substrates to Hsp104. *Mol Cell.* 2008; 32:584–591. [PubMed: 19026788]
- Toyama BH, Kelly MJ, Gross JD, Weissman JS. The structural basis of yeast prion strain variants. *Nature.* 2007; 449:233–237. [PubMed: 17767153]
- True HL, Berlin I, Lindquist SL. Epigenetic regulation of translation reveals hidden genetic variation to produce complex traits. *Nature.* 2004; 431:184–187. [PubMed: 15311209]
- True HL, Lindquist SL. A yeast prion provides a mechanism for genetic variation and phenotypic diversity. *Nature.* 2000; 407:477–483. [PubMed: 11028992]
- Tyedmers J, Madariaga ML, Lindquist S. Prion switching in response to environmental stress. *PLoS Biol.* 2008; 6:e294. [PubMed: 19067491]
- Wang H, Duennwald ML, Roberts BE, Rozeboom LM, Zhang YL, Steele AD, Krishnan R, Su LJ, Griffin D, Mukhopadhyay S, et al. Direct and selective elimination of specific prions and amyloids by 4,5-dianilinophthalimide and analogs. *Proc Natl Acad Sci USA.* 2008; 105:7159–7164. [PubMed: 18480256]
- Wegrzyn RD, Bapat K, Newnam GP, Zink AD, Chernoff YO. Mechanism of prion loss after Hsp104 inactivation in yeast. *Mol Cell Biol.* 2001; 21:4656–4669. [PubMed: 11416143]
- Weissmann C. Mutation and selection of prions. *PLoS Pathog.* 2012; 8:e1002582. [PubMed: 22479179]

Highlights

- Hsp104 disrupts intermolecular contacts of different synthetic NM prion strains
- Hsp104 selectively amplifies NM prions that confer strong [*PSI⁺*] phenotypes
- Hsp104 selectively eliminates NM prions that confer weak [*PSI⁺*] phenotypes
- Hsp104 drives strain selection events that favor prions encoding strong [*PSI⁺*]

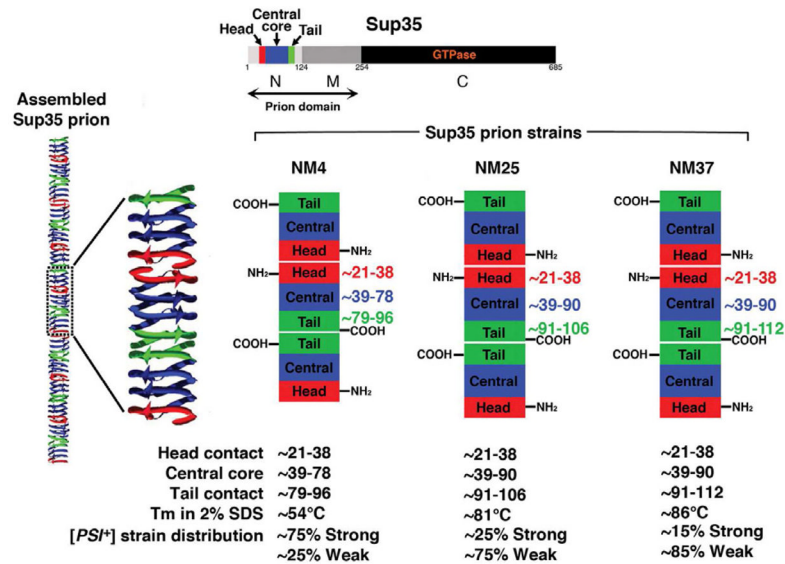


Figure 1. Chemical and biological properties of synthetic NM4, NM25, and NM37 prions
Sup35 is composed of a C-terminal GTPase domain (amino acids 254–685, black) that confers translation termination activity, a highly charged middle domain (M, amino acids 124–253, dark grey) and a prionogenic N-terminal domain (N, amino acids 1–123, light grey) enriched in glutamine, asparagine, tyrosine and glycine. Within N, prion recognition elements termed the ‘Head’ (red) and ‘Tail’ (green), which flank a ‘Central Core’ (blue), play important roles in prionogenesis. Prion recognition elements within N make homotypic intermolecular contacts such that Sup35 prions appear to be maintained by an alternating sequence of Head-to-Head (red) and Tail-to-Tail (green) contacts. The Central Core (blue) is sequestered by intramolecular contacts. Different prion strains can form depending on the environmental conditions. Thus, the NM4 prion ensemble forms at 4°C, the NM25 prion ensemble forms at 25°C, and the NM37 prion ensemble forms at 37°C. Note that on average the Central Core (blue) and Tail (green) are comprised of different amino acids in the NM4, NM25, and NM37 prion ensembles. On average, NM25 and NM37 prions have an extended central core and have a higher melting temperature in 2% SDS than NM4. Transformation of NM25 or NM37 prions into [*psi*⁻] cells yields mostly weak [*PSI*⁺], whereas transformation of NM4 prions into [*psi*⁻] cells yields mostly strong [*PSI*⁺]. These mixed distributions of weak and strong [*PSI*⁺] indicate that NM4, NM25 and NM37 are in fact complex mixtures of multiple different prion structures, rather than a single pure strain. It is also important to note that the atomic structures of Sup35 prion strains remain unknown and several models (including the models presented in this figure) have been advanced (Tessier and Lindquist, 2009).

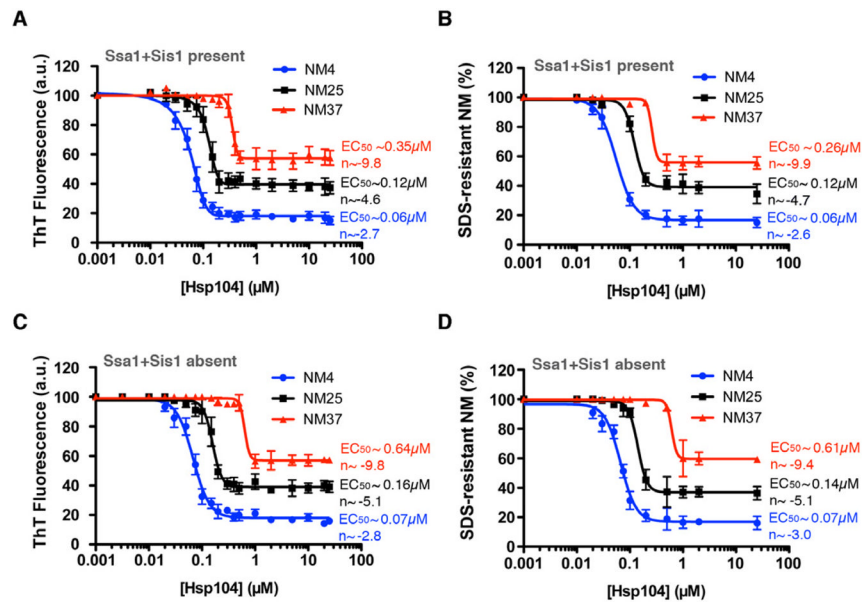


Figure 2. Hsp104 more readily remodels NM4 prions than NM25 and NM37
 (A–D) NM4, NM25, or NM37 (2.5 μ M monomer) were incubated with increasing concentrations of Hsp104 (0.001–25 μ M) in the presence (A, B) or absence (C, D) of Ssa1 (2.5 μ M) and Sis1 (2.5 μ M) for 60min at 25°C. ThT fluorescence (A, C) or SDS resistance (B, D) were used to assess prion remodeling. The EC₅₀ and Hill slope (n) are indicated next to each curve. Values represent means \pm SEM (n=2–3).

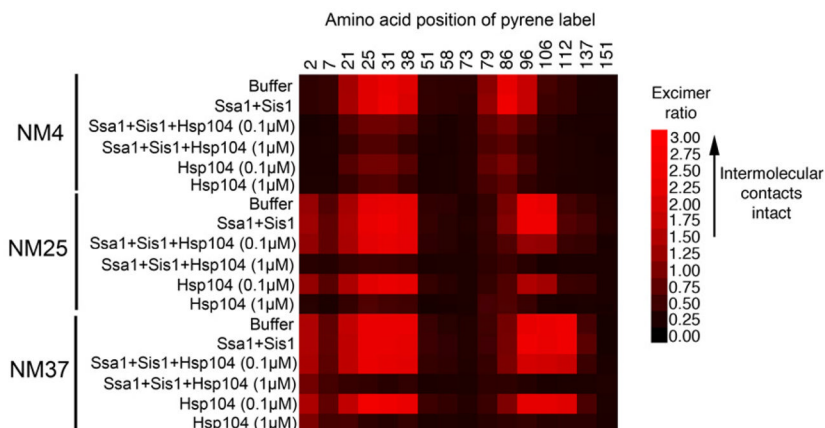


Figure 3. Hsp104 preferentially breaks NM4 intermolecular contacts at low concentrations, but preferentially disrupts NM25 and NM37 intermolecular contacts at high concentrations NM proteins (5μM) carrying pyrene labels at the indicated single site were assembled at 4°C, 25°C, or 37°C with agitation for 12h. Assembled NM4, NM25, or NM37 (2.5μM monomer) were incubated with Hsp104 (0–1μM) in the presence or absence of Ssa1 (2.5μM) and Sis1 (2.5μM) for 60min at 25°C. The ratio of excimer to non-excimer fluorescence (I_{465nm}/I_{375nm}) was then determined.

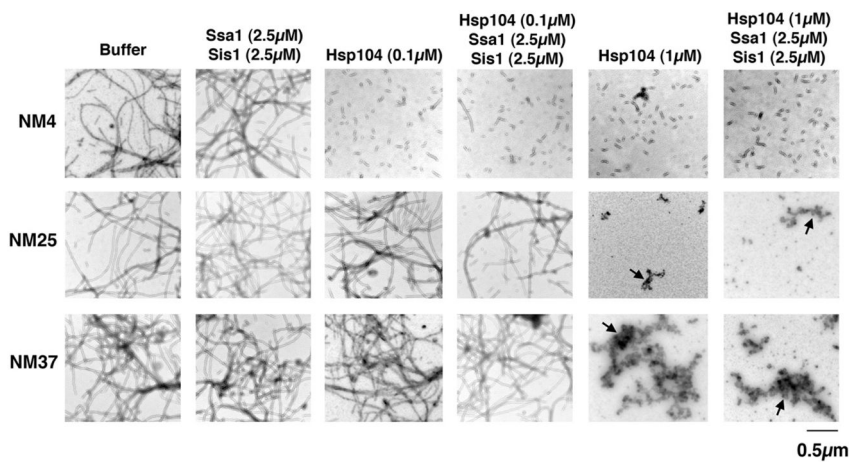


Figure 4. Hsp104 more readily fragments NM4 prions than NM25 or NM37 prions
 NM4, NM25 or NM37 (2.5μM monomer) were incubated with Hsp104 (0–1μM) in the presence or absence of Ssa1 (2.5μM) and Sis1 (2.5μM) for 60min at 25°C. Reactions were then processed for electron microscopy. Note that Hsp104 (0.1μM) more readily fragments NM4 than NM25, and NM37 is even more resistant to fragmentation. At higher Hsp104 concentration (1μM) short prion fibers persist for NM4, but NM25 and NM37 are remodeled into amorphous aggregated species (arrows). Bar, 0.5μm.

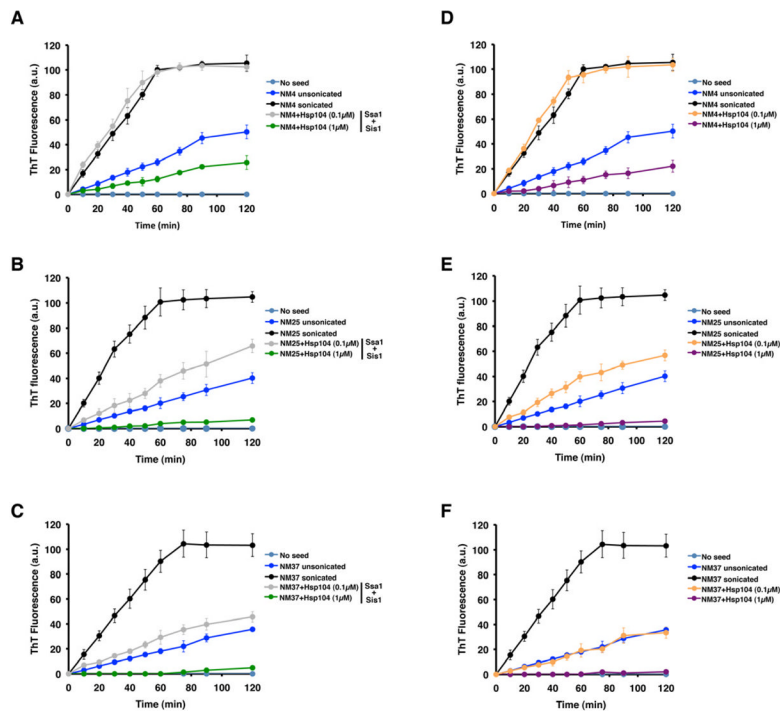


Figure 5. Hsp104 more readily eliminates the seeding activity of NM25 and NM37 prions (A–F) NM4, NM25 or NM37 (2.5 μ M monomer) were either left untreated, sonicated, or treated with His₆-Hsp104 (0.1 μ M or 1 μ M) in the presence (A–C) or absence (D–F) of Ssp1 (2.5 μ M) and Sis1 (2.5 μ M) for 60 min at 25°C. Reactions were then depleted of His₆-Hsp104 and used to seed (2% wt/wt) fresh, undisturbed NM (2.5 μ M) polymerization. Seeding reactions were performed at 4°C for NM4 products (A, D), 25°C for NM25 products (B, E), and 37°C for NM37 products (C, F). Values represent means \pm SEM (n=3).

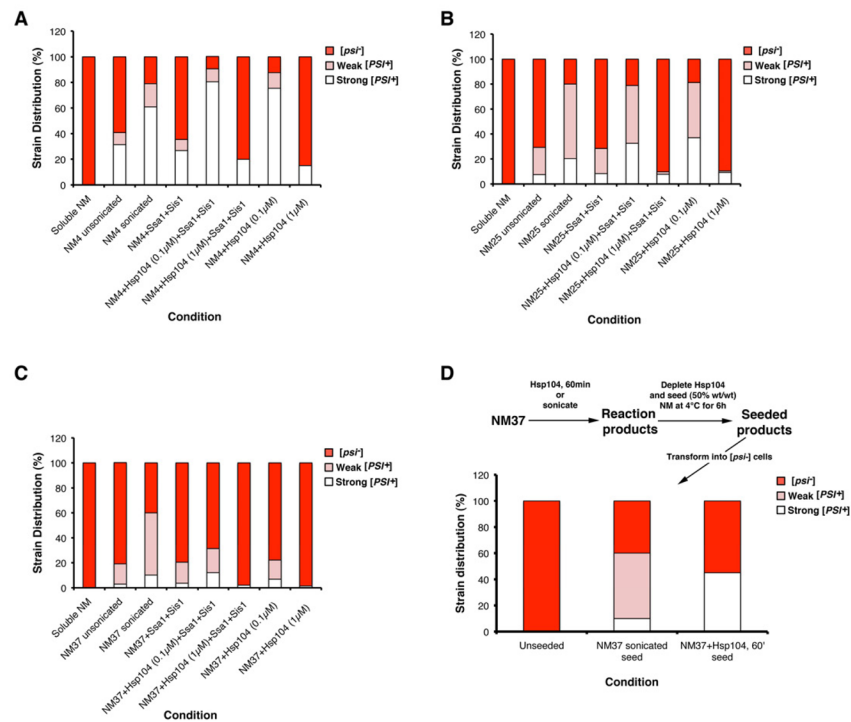


Figure 6. Hsp104 selectively amplifies prions that encode strong [*PSI*⁺] and selectively eliminates prions that encode weak [*PSI*⁺] in vitro

(A–C) NM4 (A), NM25 (B) or NM37 (C) (2.5 μM monomer) were either left untreated, sonicated, or treated with His₆-Hsp104 (0.1 μM or 1 μM) in the presence or absence of Ssa1 (2.5 μM) and Sis1 (2.5 μM) for 60 min at 25°C. Reactions were then depleted of His₆-Hsp104, concentrated and transformed into [*psi*⁻] cells. Soluble NM served as a negative control. The number of weak and strong [*PSI*⁺] colonies relative to total transformants was then determined. Values represent means from three experiments.

(D) NM37 (2.5 μM monomer) were either sonicated or treated with His₆-Hsp104 (1 μM), Ssa1 (2.5 μM), and Sis1 (2.5 μM) for 60 min at 25°C. Reactions were then depleted of His₆-Hsp104 and used to seed (50% wt/wt) fresh, undisturbed NM (2.5 μM) polymerization at 4°C for 6 h. Unseeded reactions served as a control. Reaction products were concentrated, sonicated and transformed into [*psi*⁻] cells. Soluble NM served as a negative control. The number of weak and strong [*PSI*⁺] colonies relative to total transformants was then determined. Values represent means from three experiments.

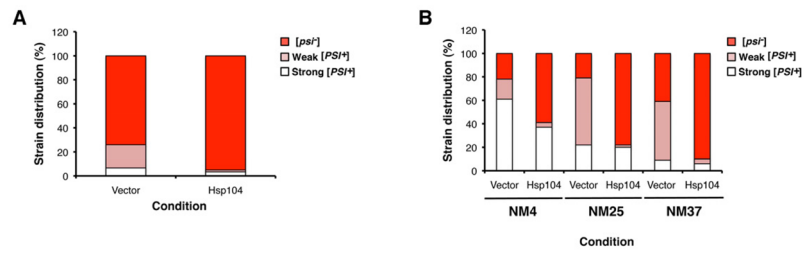


Figure 7. Hsp104 selectively amplifies prions that encode strong [*PSI*⁺] and selectively eliminates prions that encode weak [*PSI*⁺] in vivo

(A) NM-YFP was overexpressed for 6h at 30°C in [*psi*⁻] [*PIN*⁺] cells expressing normal (vector) or elevated (Hsp104) levels of Hsp104. Cells were plated on 25% YPD and the proportion of [*psi*⁻], weak [*PSI*⁺], and strong [*PSI*⁺] colonies was determined. Values represent means from three experiments.

(B) NM4, NM25, or NM37 were transformed into [*psi*⁻] cells expressing normal (vector) or elevated levels of Hsp104 (Hsp104). The number of weak and strong [*PSI*⁺] colonies relative to total transformants was then determined. Values represent means from three experiments.